ATLAS and CMS results on CP-Violation: new results & prospects

Radek Novotný
on behalf of the ATLAS and CMS collaborations

SM@LHC 2021, CERN
April 29, 2021

Motivation

- $B_s^0 \to J/\psi\phi$ is used to measure the CP-violating phase ϕ_s which is potentially sensitive to NP
- The CP violation occurs due to interference between a direct decay and a decay with $B_s^0 - \bar{B}_s^0$ mixing
- In the SM ϕ_s is related to the CKM elements and predicted with high precision
  $\phi_s \simeq 2\arg[-(V_{ts}V_{tb}^*)/(V_{cs}V_{cb}^*)] = -0.03696^{+0.00072}_{-0.00082}$ rad

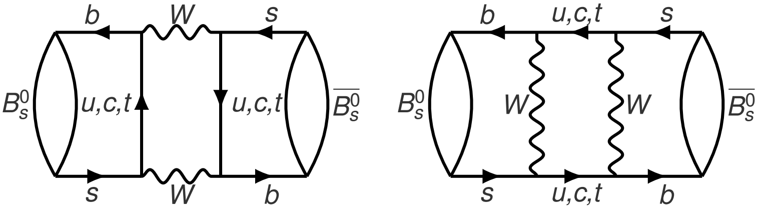

- The other quantity in B_s^0 mixing is $\Delta\Gamma_s = \Gamma_s^L - \Gamma_s^H$, where Γ_s^L and Γ_s^H are the decay widths of the different mass eigenstates. $\Delta\Gamma_s$ is not sensitive to New Physics, however measurement is interesting to test the theory. The theory prediction is $\Delta\Gamma = (0.091 \pm 0.013)\,\mathrm{ps}^{-1}$
- The New Physics processes could introduce additional contributions to the box diagrams describing the B_s^0 mixing

Status before LHC Run2

- The CP-violation measurement in the $B_s^0 \to J/\psi\phi$ channel was previously performed at the LHC in Run1 and at the Tevatron CDF and $D\emptyset$ experiments.
- The results were consistent with the SM prediction within measured uncertainties.
- Although large new physics enhancements of the mixing amplitude have been excluded by the precise measurement of the oscillation frequency, there is still room for improvements and discoveries

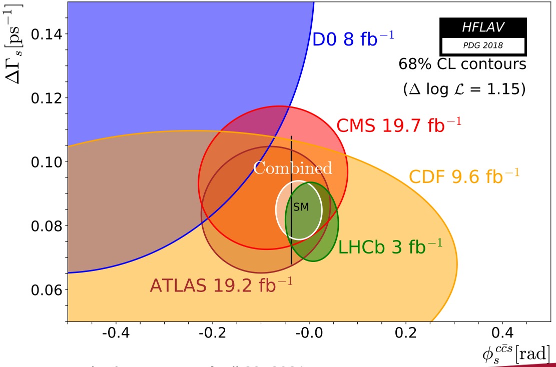

HFLAV Collaboration

ATLAS and CMS measurements in LHC Run2

ATLAS

Eur. Phys. J. C 81 (2021) 342

- $\sqrt{s} = 13$ TeV collected between years 2015 and 2017 corresponding to 80.5 fb^{-1}
- Events collected with mixture of triggers based on $J/\psi \to \mu^+\mu^-$ identification, with muon p_T thresholds of either 4 GeV or 6 GeV (vary over run periods)
- No lifetime or impact parameter cut at trigger level

CMS

Phys. Lett. B 816 (2021) 136188

- $\sqrt{s} = 13$ TeV collected between years 2017 and 2018 corresponding to 96.4 fb^{-1}
- The trigger requires three muons, with the minimum p_T requirement on the highest p_T (leading, μ_1) and second-highest p_T (subleading, μ_2) muons of $p_\mathrm{T} > 5$ and 3 GeV, respectively, and the dimuon invariant mass $m_{\mu_1\mu_2} < 9$ GeV.
- Proper decay length cut $ct > 70$ µm

- $B_s^0 \to J/\psi\phi$ = pseudoscalar to vector-vector
- Final state: admixture of CP-odd ($L = 1$) and CP-even ($L = 0, 2$) states
- Distinguishable through time-dependent angular analysis
- Non-resonant S-wave decay $B_s^0 \to J/\psi K^+ K^-$ contributes to the final state
- Included in the differential decay rate due to interference with the $B_s^0 \to J/\psi(\mu^+\mu^-)\phi(K^+K^-)$ decay

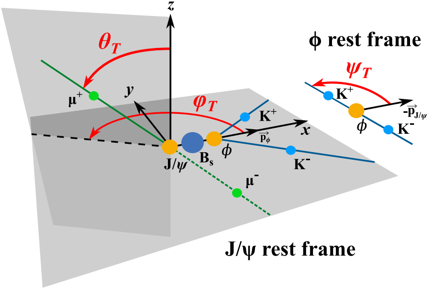

Figure: Angles between final state particles in transversity basis.

Mass-lifetime-angular fit

An unbinned maximum-likelihood fit is performed on the combined data samples extracting parameters of interest:

- CPV phase ϕ_s
- Decay widths: $\Delta\Gamma_s$, $\Gamma_s = \frac{\Gamma_L+\Gamma_H}{2}$
- The size of the CP-state amplitudes at $t = 0$: $|A_0(0)|^2$, $|A_{\|}(0)|^2$ (ATLAS), $|A_{\perp}(0)|^2$ (CMS), $|A_S(0)|^2$

$$|A_0(0)|^2 + |A_{\|}(0)|^2 + |A_{\perp}(0)|^2 = 1$$

- The strong phases $\delta_{\|}$, $\delta_{\perp}$, δ_S, $\delta_0 = 0$ (CMS $\delta_{S\perp} = \delta_S - \delta_{\perp}$)
- $\Delta m_s = |m_L - m_H|$ (ATLAS uses value fixed to PDG $\Delta m_s = 17.77\,\mathrm{ps}^{-1}$)
- $|\lambda|$ (ATLAS uses value fixed to 1.0)

Flavour tagging

- Opposite side tagging
  - Use $b - \bar{b}$ pair correlation to infer initial signal flavour from the other B meson
  - Provide the probability of signal candidate to be B_s^0 or $\overline{B}_s^0$
- Semileptonic Tagging method
  - $b \to l$ transitions are clean tagging method
  - $b \to c \to l$ and neutral B-meson oscillations dilute the tagging
- Jet-Charge
  - Information from tracks in b-tagged jets
- Calibration using $B^{\pm} \to J/\psi K^{\pm}$
  - Self-tagging, non-oscillating channel
- Tagging methods used:
  - ATLAS : tight muon[1], electron, low-p_{T} muon[2], jet
  - CMS : muon

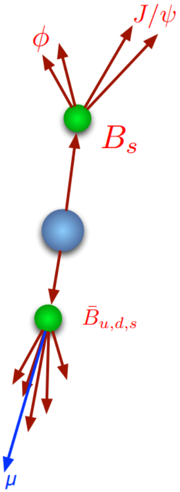

[1] Tight muon reconstruction is optimised to maximise the purity of muons at the cost of some efficiency.
[2] This working point is optimised to provide good muon reconstruction efficiency down to a p_{T} of ≈ 3 GeV, while controlling the fake-muon rate.

Tagging performance

- The probability to tag a B_s^0 meson as containing a $\bar{b}$-quark:

$$P(B|Q) = \frac{P(Q|B^+)}{P(Q|B^+) + P(Q|B^-)}$$

- **Efficiency**: Fraction of signals with specific tagger, $\varepsilon = \frac{N_{\text{tagged}}}{N_{\text{Bcand}}}$
- **Dilution**: $D = (1 - 2\omega)$, where ω is the mistag probability that is defined as ratio between the number of wrongly tagged events and the total number of tagged events
- **Tagging Power**: figure of merit of tagger performance
    - Depends on dilution and efficiency:

$$P = T = \varepsilon D^2 = \varepsilon(1 - 2\omega)^2$$

CMS

Data sample	ε_{tag} (%)	ω_{tag} (%)	P_{tag} (%)
2017	45.7 ± 0.1	27.1 ± 0.1	9.6 ± 0.1
2018	50.9 ± 0.1	27.3 ± 0.1	10.5 ± 0.1

ATLAS

Tag method	ϵ_x [%]	D_x [%]	T_x [%]
Tight muon	4.50 ± 0.01	43.8 ± 0.2	0.862 ± 0.009
Electron	1.57 ± 0.01	41.8 ± 0.2	0.274 ± 0.004
Low-p_{T} muon	3.12 ± 0.01	29.9 ± 0.2	0.278 ± 0.006
Jet	12.04 ± 0.02	16.6 ± 0.1	0.334 ± 0.006
Total	21.23 ± 0.03	28.7 ± 0.1	1.75 ± 0.01

Systematic uncertainties

- Extensive systematic studies were performed by both experiments
- Here is the list of the major contributions to the total systematics:

ATLAS

- **Flavour tagging:** calibration, $B_s^0 - B^{\pm}$ MC difference and dependencies on the pile-up distribution
- **Fit bias:** fit stability is validated by the pseudo-experiments with default fit results
- **Background angles model:** varying the bin boundaries, invariant mass window and sideband definition
- **Best candidate selection:** statistically equivalent sample is created where all candidates in the event are retained
- **Angular acceptance method:** different acceptance functions are calculated using different numbers of p_{T} bins as well as different widths and central values of the bins

CMS

- **Model bias:** pseudo experiments, each statistically equivalent to the data samples, from the fitted model in data
- **Angular efficiency:** systematic uncertainty related to the limited MC event count used to estimate the angular efficiency function is evaluated by regenerating the efficiency histograms
- **Proper decay length resolution:** varying the κ correction factor by $\pm 10\%$, as estimated from a data-to-simulation comparison
- **Sig./bkg. ω_{evt} difference:** differences in the mistag probabilities between signal and background studied on the sideband and signal range

ATLAS

- ATLAS found two well-separated local maxima of the likelihood for the strong-phases $\delta_{\parallel}$ and $\delta_{\perp}$

Parameter	Value	Statistical uncertainty	Systematic uncertainty
ϕ_s [rad]	–0.081	0.041	0.022
$\Delta\Gamma_s$ [ps^{-1}]	0.0607	0.0047	0.0043
Γ_s [ps^{-1}]	0.6687	0.0015	0.0022
$\|A_{\parallel}(0)\|^2$	0.2213	0.0019	0.0023
$\|A_0(0)\|^2$	0.5131	0.0013	0.0038
$\|A_S(0)\|^2$	0.0321	0.0033	0.0046
$\delta_{\perp} - \delta_S$ [rad]	–0.25	0.05	0.04
Solution (a)			
$\delta_{\perp}$ [rad]	3.12	0.11	0.06
$\delta_{\parallel}$ [rad]	3.35	0.05	0.09
Solution (b)			
$\delta_{\perp}$ [rad]	2.91	0.11	0.06
$\delta_{\parallel}$ [rad]	2.94	0.05	0.09

CMS

Parameter	Fit value	Stat. uncer.	Syst. uncer.
ϕ_s [mrad]	-11	± 50	± 10
$\Delta\Gamma_s$ [ps^{-1}]	0.114	± 0.014	± 0.007
Δm_s [$\hbar$ ps^{-1}]	17.51	$^{+0.10}_{-0.09}$	± 0.03
$\|\lambda\|$	0.972	± 0.026	± 0.008
Γ_s [ps^{-1}]	0.6531	± 0.0042	± 0.0024
$\|A_0\|^2$	0.5350	± 0.0047	± 0.0048
$\|A_{\perp}\|^2$	0.2337	± 0.0063	± 0.0044
$\|A_S\|^2$	0.022	$^{+0.008}_{-0.007}$	± 0.016
$\delta_{\parallel}$ [rad]	3.18	± 0.12	± 0.03
$\delta_{\perp}$ [rad]	2.77	± 0.16	± 0.04
$\delta_{S\perp}$ [rad]	0.221	$^{+0.083}_{-0.070}$	± 0.048

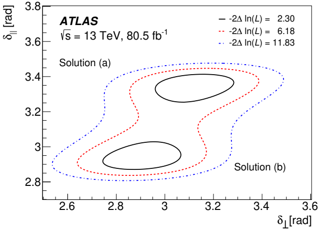

Combination with Run1 results

- Both experiments performed a statistical combination of their new results with those obtained in Run1 using the BLUE method. This method uses the measured values and uncertainties of the parameters as well as the correlations between them

$$\phi_s = -87 \pm 36(\text{stat.}) \pm 21(\text{syst.})\,\text{mrad},$$
$$\Delta\Gamma_s = 0.0657 \pm 0.0043(\text{stat.}) \pm 0.0037(\text{syst.})\,\text{ps}^{-1}$$

$$\phi_s = -21 \pm 44(\text{stat.}) \pm 10(\text{syst.})\,\text{mrad},$$
$$\Delta\Gamma_s = 0.1032 \pm 0.0095(\text{stat.}) \pm 0.0048(\text{syst.})\,\text{ps}^{-1}$$

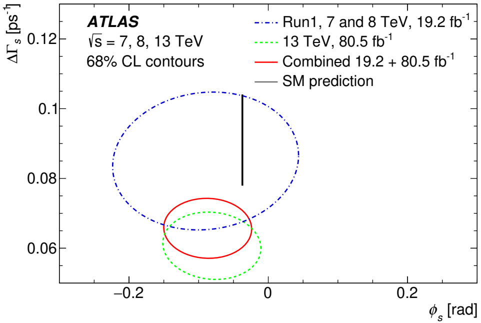

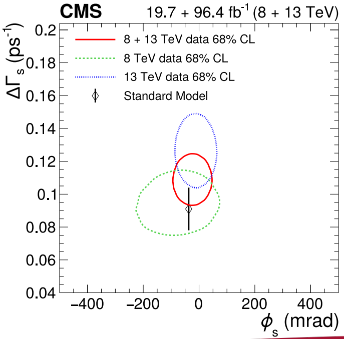

Comparison in $\Delta\Gamma_s - \phi_s$ plane

- Two-dimensional likelihood contours in the $\Delta\Gamma_s - \phi_s$ plane include the latest LHCb results from LHC Run2 (EPJC 80, 601 (2020))
- Experiments are consistent with each other and with the SM prediction, however some tension occurs in other parameters especially in Γ_s ($\sim 3\sigma$ tension)

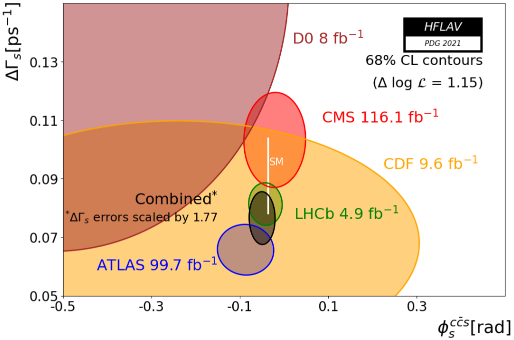

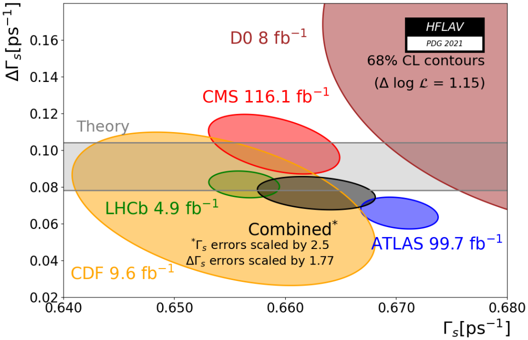

Summary and outlook

- ATLAS and CMS performed analysis on the latest LHC Run2 data
- Both experiments are consistent with their Run1 results and with SM predictions

- ATLAS is working on the full Run2 measurement (additional 60 fb^{-1} from 2018) with updated fit model that include the extraction of Δm_s and $|\lambda|$ parameters
- CMS is working on the measurement with full Run2 statistics with more general triggers that do not require 3rd muon in the event, and they plan also to use more tagging methods (electron, jet)

- Preparations for Run3 are very active, especially on the trigger side, to ensure a large amount of high quality data

Summary and outlook

- ATLAS and CMS performed analysis on the latest LHC Run2 data
- Both experiments are consistent with their Run1 results and with SM predictions

- ATLAS is working on the full Run2 measurement (additional 60 fb^{-1} from 2018) with updated fit model that include the extraction of Δm_s and $|\lambda|$ parameters
- CMS is working on the measurement with full Run2 statistics with more general triggers that do not require 3rd muon in the event, and they plan also to use more tagging methods (electron, jet)

- Preparations for Run3 are very active, especially on the trigger side, to ensure a large amount of high quality data

Thanks for your attention!

Backup slides.

Likelihood fit function (by ATLAS)

$$\ln \mathcal{L} = \sum_{i=1}^{N} \{ \underbrace{w_i}_{\text{Tau weight}} \cdot \ln(\underbrace{f_s \cdot \mathcal{F}_s}_{\text{Signal}} + \underbrace{f_s \cdot f_{B_d^0} \cdot \mathcal{F}_{B_d^0} + f_s \cdot f_{\Lambda_b} \cdot \mathcal{F}_{\Lambda_b}}_{\text{Peaking background}} + \underbrace{(1 - f_s \cdot (1 + f_{B_d^0} + f_{\Lambda_b})) \cdot \mathcal{F}_{\text{bkg}}}_{\text{Combinatorial background}}) \}$$

- Data are corrected by the decay time correction
- Mass as well as lifetime use per-candidate width and scale factor, with flavour-dependent terms weighted by tagging probability $P(B|Q)$
- Contributions from $B_d^0 \to J/\psi K^{*0}$, $B_d^0 \to J/\psi K\pi$ and $\Lambda_b^0 \to J/\psi Kp$ due to wrong mass assignment (KK)
  - Efficiencies and acceptance from MC
  - BR from PDG
  - Fragmentation fractions from other measurements
- Combinatorial background for angular distribution use Legendre polynomials from sidebands; fixed in the main fit

Time-Angular signal PDF (by ATLAS)

k	$O^{(k)}(t)$	$g^{(k)}(\theta_T,\psi_T,\phi_T)$
1	$\frac{1}{2}\lvert A_0(0)\rvert^2\left[(1+\cos\phi_s)\,e^{-\Gamma_L^{(s)}t}+(1-\cos\phi_s)\,e^{-\Gamma_H^{(s)}t}\pm 2e^{-\Gamma_s t}\sin(\Delta m_s t)\sin\phi_s\right]$	$2\cos^2\psi_T(1-\sin^2\theta_T\cos^2\phi_T)$
2	$\frac{1}{2}\lvert A_\parallel(0)\rvert^2\left[(1+\cos\phi_s)\,e^{-\Gamma_L^{(s)}t}+(1-\cos\phi_s)\,e^{-\Gamma_H^{(s)}t}\pm 2e^{-\Gamma_s t}\sin(\Delta m_s t)\sin\phi_s\right]$	$\sin^2\psi_T(1-\sin^2\theta_T\sin^2\phi_T)$
3	$\frac{1}{2}\lvert A_\perp(0)\rvert^2\left[(1-\cos\phi_s)\,e^{-\Gamma_L^{(s)}t}+(1+\cos\phi_s)\,e^{-\Gamma_H^{(s)}t}\mp 2e^{-\Gamma_s t}\sin(\Delta m_s t)\sin\phi_s\right]$	$\sin^2\psi_T\sin^2\theta_T$
4	$\frac{1}{2}\lvert A_0(0)\rvert\lvert A_\parallel(0)\rvert\cos\delta_\parallel\left[(1+\cos\phi_s)\,e^{-\Gamma_L^{(s)}t}+(1-\cos\phi_s)\,e^{-\Gamma_H^{(s)}t}\pm 2e^{-\Gamma_s t}\sin(\Delta m_s t)\sin\phi_s\right]$	$\frac{1}{\sqrt{2}}\sin 2\psi_T\sin^2\theta_T\sin 2\phi_T$
5	$\lvert A_\parallel(0)\rvert\lvert A_\perp(0)\rvert\left[\frac{1}{2}(e^{-\Gamma_L^{(s)}t}-e^{-\Gamma_H^{(s)}t})\cos(\delta_\perp-\delta_\parallel)\sin\phi_s\pm e^{-\Gamma_s t}(\sin(\delta_\perp-\delta_\parallel)\cos(\Delta m_s t)-\cos(\delta_\perp-\delta_\parallel)\cos\phi_s\sin(\Delta m_s t))\right]$	$-\sin^2\psi_T\sin 2\theta_T\sin\phi_T$
6	$\lvert A_0(0)\rvert\lvert A_\perp(0)\rvert\left[\frac{1}{2}(e^{-\Gamma_L^{(s)}t}-e^{-\Gamma_H^{(s)}t})\cos\delta_\perp\sin\phi_s\pm e^{-\Gamma_s t}(\sin\delta_\perp\cos(\Delta m_s t)-\cos\delta_\perp\cos\phi_s\sin(\Delta m_s t))\right]$	$\frac{1}{\sqrt{2}}\sin 2\psi_T\sin 2\theta_T\cos\phi_T$
7	$\frac{1}{2}\lvert A_S(0)\rvert^2\left[(1-\cos\phi_s)\,e^{-\Gamma_L^{(s)}t}+(1+\cos\phi_s)\,e^{-\Gamma_H^{(s)}t}\mp 2e^{-\Gamma_s t}\sin(\Delta m_s t)\sin\phi_s\right]$	$\frac{2}{3}\left(1-\sin^2\theta_T\cos^2\phi_T\right)$
8	$\alpha\lvert A_S(0)\rvert\lvert A_\parallel(0)\rvert\left[\frac{1}{2}(e^{-\Gamma_L^{(s)}t}-e^{-\Gamma_H^{(s)}t})\sin(\delta_\parallel-\delta_S)\sin\phi_s\pm e^{-\Gamma_s t}(\cos(\delta_\parallel-\delta_S)\cos(\Delta m_s t)-\sin(\delta_\parallel-\delta_S)\cos\phi_s\sin(\Delta m_s t))\right]$	$\frac{1}{3}\sqrt{6}\sin\psi_T\sin^2\theta_T\sin 2\phi_T$
9	$\frac{1}{2}\alpha\lvert A_S(0)\rvert\lvert A_\perp(0)\rvert\sin(\delta_\perp-\delta_S)\left[(1-\cos\phi_s)\,e^{-\Gamma_L^{(s)}t}+(1+\cos\phi_s)\,e^{-\Gamma_H^{(s)}t}\mp 2e^{-\Gamma_s t}\sin(\Delta m_s t)\sin\phi_s\right]$	$\frac{1}{3}\sqrt{6}\sin\psi_T\sin 2\theta_T\cos\phi_T$
10	$\alpha\lvert A_0(0)\rvert\lvert A_S(0)\rvert\left[\frac{1}{2}(e^{-\Gamma_H^{(s)}t}-e^{-\Gamma_L^{(s)}t})\sin\delta_S\sin\phi_s\pm e^{-\Gamma_s t}(\cos\delta_S\cos(\Delta m_s t)+\sin\delta_S\cos\phi_s\sin(\Delta m_s t))\right]$	$\frac{4}{3}\sqrt{3}\cos\psi_T\left(1-\sin^2\theta_T\cos^2\phi_T\right)$

Fit projections (by ATLAS)

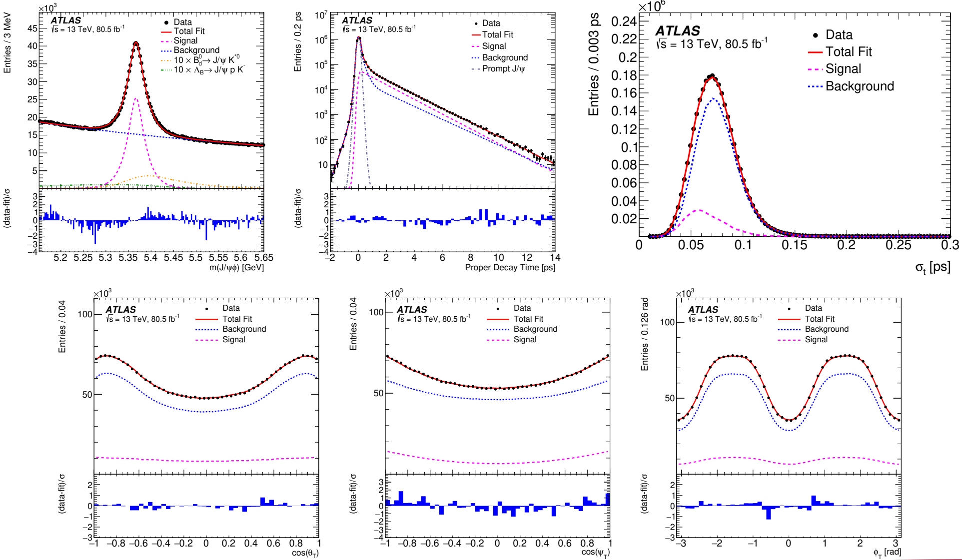

Fit projections (by CMS)

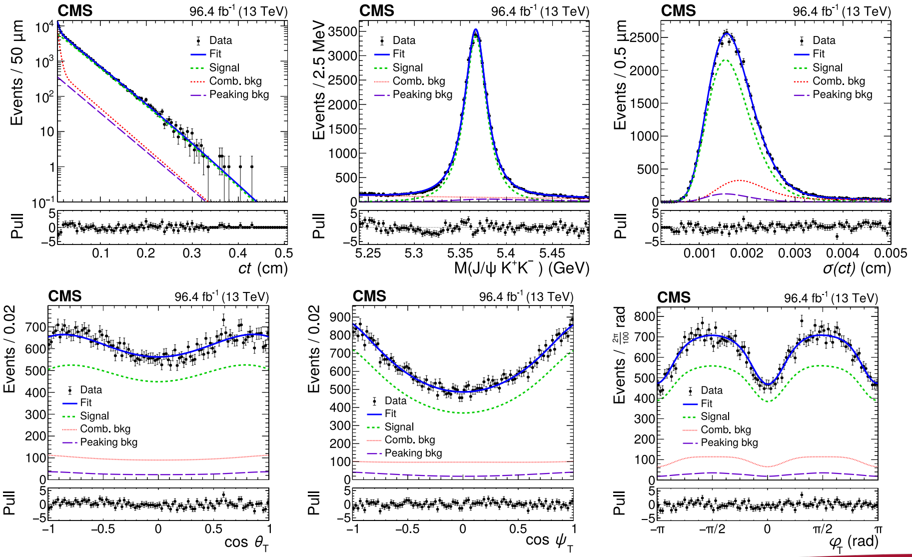

Systematic table (by ATLAS)

	ϕ_s [10^{-3} rad]	$\Delta\Gamma_s$ [10^{-3} ps^{-1}]	Γ_s [10^{-3} ps^{-1}]	$\|A_\parallel(0)\|^2$ [10^{-3}]	$\|A_0(0)\|^2$ [10^{-3}]	$\|A_S(0)\|^2$ [10^{-3}]	$\delta_\perp$ [10^{-3} rad]	$\delta_\parallel$ [10^{-3} rad]	$\delta_\perp - \delta_S$ [10^{-3} rad]
Tagging	19	0.4	0.3	0.2	0.2	1.1	17	19	2.3
ID alignment	0.8	0.2	0.5	< 0.1	< 0.1	< 0.1	11	7.2	< 0.1
Acceptance	0.5	0.3	< 0.1	1.0	0.9	2.9	37	64	8.6
Time efficiency	0.2	0.2	0.5	< 0.1	< 0.1	0.1	3.0	5.7	0.5
Best candidate selection	0.4	1.6	1.3	0.1	1.0	0.5	2.3	7.0	7.4
Background angles model:									
Choice of fit function	2.5	< 0.1	0.3	1.1	< 0.1	0.6	12	0.9	1.1
Choice of p_T bins	1.3	0.5	< 0.1	0.4	0.5	1.2	1.5	7.2	1.0
Choice of mass window	9.3	3.3	< 0.1	0.4	0.8	0.4	17	8.6	1.8
Choice of sidebands intervals	0.4	0.1	0.1	0.3	0.3	1.3	4.4	7.4	2.3
Dedicated backgrounds:									
B_d^0	2.6	1.1	< 0.1	0.2	3.1	1.5	10	23	2.1
Λ_b	1.6	0.3	0.2	0.5	1.2	1.8	14	30	0.8
Alternate Δm_s	1.0	< 0.1	< 0.1	< 0.1	< 0.1	< 0.1	15	4.0	< 0.1
Fit model:									
Time res. sig frac	1.4	1.1	0.5	0.5	0.6	0.8	12	30	0.4
Time res. p_T bins	0.7	0.5	0.8	0.1	0.1	0.1	2.2	14	0.7
S-wave phase	0.3	< 0.1	< 0.1	< 0.1	< 0.1	0.2	8.0	15	37
Fit bias	5.7	1.3	1.2	1.3	0.4	1.1	3.3	19	0.3
Total	22	4.3	2.2	2.3	3.8	4.6	55	88	39

Systematic table (by CMS)

	ϕ_s [mrad]	$\Delta\Gamma_s$ [ps^{-1}]	Δm_s [$\hbar$ ps^{-1}]	$\|\lambda\|$	Γ_s [ps^{-1}]	$\|A_0\|^2$	$\|A_\perp\|^2$	$\|A_S\|^2$	$\delta_\parallel$ [rad]	$\delta_\perp$ [rad]	$\delta_{S\perp}$ [rad]
Statistical uncertainty	50	0.014	0.10	0.026	0.0042	0.0047	0.0063	0.0077	0.12	0.16	0.083
Model bias	7.9	0.0019	—	0.0035	0.0005	0.0002	0.0012	0.001	0.020	0.016	0.006
Angular efficiency	3.8	0.0006	0.007	0.0057	0.0002	0.0008	0.0010	0.002	0.006	0.015	0.015
Proper decay length efficiency	0.3	0.0062	0.001	0.0002	0.0022	0.0014	0.0023	0.001	0.001	0.002	0.002
Proper decay length resolution	2.5	0.0008	0.015	0.0009	0.0005	0.0007	0.0009	0.007	0.006	0.025	0.022
Data/simulation difference	0.6	0.0008	0.004	0.0003	0.0003	0.0044	0.0029	0.007	0.007	0.007	0.028
Flavor tagging	0.1	$<10^{-4}$	0.001	0.0002	$<10^{-4}$	0.0003	$<10^{-4}$	$<10^{-3}$	0.001	0.003	0.001
Sig./bkg. ω_{evt} difference	3.0	—	—	—	0.0005	—	0.0008	—	—	—	0.006
Model assumptions	—	0.0008	—	0.0046	0.0003	—	0.0013	0.001	0.017	0.019	0.011
Peaking background	0.3	0.0008	0.011	$<10^{-4}$	0.0002	0.0005	0.0002	0.003	0.005	0.007	0.011
S-P wave interference	—	0.0010	0.019	—	0.0005	0.0005	—	0.013	—	0.019	0.019
Total systematic uncertainty	9.6	0.0067	0.028	0.0082	0.0024	0.0048	0.0044	0.016	0.028	0.045	0.047

Calibration of the per-event mistag probability (by CMS)

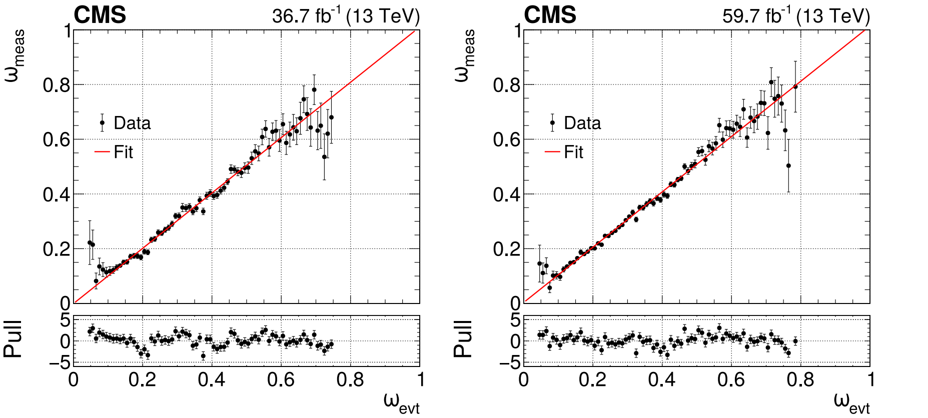

Figure: Results of the calibration of the per-event mistag probability ω_{evt} based on $B^{\pm} \to J/\psi K^{\pm} \to \mu^{+}\mu^{-}K^{\pm}$ decays from the 2017 (left) and 2018 (right) data samples. The vertical bars represent the statistical uncertainties. The solid line shows a linear fit to data (solid markers). The pull distributions between the data and the fit function in each bin are shown in the lower panels.